Inorg. Chem. **2008**, *47*, 4564−4569

Self-Encapsulation of $[M^{II}(phen)_2(H_2O)_2]^{2+}$ (M = Co, Zn) in One-Dimensional Nanochannels of $[M^{II}(H_2O)_6(BTC)_2]^{4-}$ (M = Co, Cu, Mn): A High HQ/CAT Ratio Catalyst for Hydroxylation of Phenols

Jianhong Bi,*,† Lingtao Kong,‡ Zixiang Huang,§ and Jinhuai Liu‡

Department of Chemistry, Hefei Teachers College, 327 Jinzhai Road, Hefei 230061, P. R. China, Hefei Institute of Intelligent Machines, Chinese Academy of Sciences, P.O. Box 1130, Hefei 230031, P. R. China, and Fujian Institute of Research on the Structure of Matter, Chinese Academy of Sciences, 155 YangQiao West Road, Fuzhou 350002, P. R. China

Received November 9, 2007

Four novel three-dimensional (3D) microporous supramolecular compounds containing nanosized channels, namely, $[Co(phen)_2(H_2O)_2]_2[Co(H_2O)_6]\cdot 2BTC\cdot 21.5H_2O$ (**1**), $[Co(phen)_2(H_2O)_2]_2[Cu(H_2O)_6]\cdot 2BTC\cdot 21.5H_2O$ (**2**), $[Co(phen)_2(H_2O)_2]_2[Mn(H_2O)_6]\cdot 2BTC\cdot 18H_2O$ (**3**), and $[Zn(phen)_2(H_2O)_2]_2[Mn(H_2O)_6]\cdot 2BTC\cdot 22.5H_2O$ (**4**), were synthesized from 1,3,5-benzenetricarboxylate (BTC), 1,10-phenanthroline (phen), and the transition-metal salt(s) by self-assembly. Single-crystal X-ray structural analysis showed that the resulting 3D microporous supramolecular frameworks consist of a two-dimensional (2D) hydrogen-bonded host framework of $[M^{II}(H_2O)_6(BTC)_2]^{4-}$ (M = Co for **1**, Cu for **2**, Mn for **3**, **4**) with rectangular-shaped cavities containing $[M^{II}(phen)_2(H_2O)_2]^{2+}$ (M = Co for **1**−**3**, Zn for **4**) guests. The guest complex is encapsulated in the 2D hydrogen-bonded host framework by hydrogen bonding and aromatic $\pi-\pi$ stacking interactions, forming the 3D hydrogen-bonded framework. The catalytic activities of **1**, **2**, **3**, and **4** were studied using hydroxylation of phenols with 30% aqueous H_2O_2 as a test reaction. The compounds displayed a good phenol conversion ratio and excellent channel selectivity in the hydroxylation reaction, with a maximum hydroquinone (HQ)/catechol (CAT) ratio of 3.9.

Introduction

Microporous inorganic materials, including zeolites, aluminum phosphates, and transition-metal phosphates, are particularly important for their applications as molecular sieves, desiccants, ion exchangers, and catalysts,[1–4] and thus, they have been studied in detail in the past decades. Several years ago, the family of microporous compounds was extended to metal−organic frameworks (MOFs), or coordination polymers.[5–7] Compared with inorganic compounds, MOFs built from molecular building blocks hold great promise for their ease of processability, flexibility, structural diversity, and geometrical control over size, shape, and symmetry.[8–11] However, few catalytically active MOFs have been constructed, because the metal ions and the ligands are usually selected for suitability as building blocks of the MOFs rather than as catalysts. As a result, most MOFs have no potential catalytic activity, and few catalytically active MOFs have been exploited.[12–14] Given that zeolites having metal complexes encapsulated in their matrix cavities

* To whom correspondence should be addressed. E-mail: hxx010101@126.com. Tel: +86-551-2826176. Fax: +86-551-3674252.
† Hefei Teachers College.
‡ Hefei Institute of Intelligent Machines, Chinese Academy of Sciences.
§ Fujian Institute of Research on the Structure of Matter, Chinese Academy of Sciences.

(1) Gier, T. E.; Stucky, G. D. *Nature* **1991**, *349*, 508–510.
(2) Wilson, S. T.; Lok, B. M.; Messina, C. A.; Cannan, T. R.; Flanigen, E. M. *J. Am. Chem. Soc.* **1982**, *104*, 1146–1147.
(3) Gier, T. E.; Bu, X.; Feng, P.; Stucky, G. D. *Nature* **1998**, *395*, 154–157.
(4) Feng, P.; Bu, X.; Stucky, G. D. *Nature* **1997**, *388*, 735–741.
(5) Yaghi, O. M.; Li, H.-L.; Davis, C.; Richardson, D.; Groy, T. L. *Acc. Chem. Res.* **1998**, *31*, 474–484.
(6) Chen, B.; Ma, S.; Zapata, F.; Fronczek, F. R.; Lobkovsky, E. B.; Zhou, H.-C. *Inorg. Chem.* **2007**, *46*, 1233–1236.
(7) Custelcean, R.; Haverlock, T. J.; Moyer, B. A. *Inorg. Chem.* **2006**, *45*, 6446–6452.
(8) Muller, U.; Schubert, M.; Teich, F.; Puetter, H.; Schierle-Arndt, K.; Pastré, J. *J. Mater. Chem.* **2006**, *16*, 626–636.
(9) Liang, J.; Shimizu, G. K. H. *Inorg. Chem.* **2007**, *46*, 10449–10451.
(10) Rowsell, J. L. C.; Yaghi, O. M. *J. Am. Chem. Soc.* **2006**, *128*, 1304–1315.
(11) Tran, D. T.; Fan, X.; Brennan, D. P.; Zavalij, P. Y.; Oliver, S. R. J. *Inorg. Chem.* **2005**, *44*, 6192–6196.
(12) Fujita, M.; Kwon, Y. J.; Washizu, S.; Ogura, K. *J. Am. Chem. Soc.* **1994**, *116*, 1151–1152.

10.1021/ic7022049 CCC: $40.75
Published on Web 04/26/2008

possess the advantages of solid heterogeneous catalysts,[15–18] we considered whether it would be possible to manufacture similar catalysts by encapsulating a metal complex $[M^{II}(phen)_2(H_2O)_2]^{2+}$ (M = Co, Zn) as a catalytic activity center into a $[M^{II}(H_2O)_6(BTC)_2]^{4-}$ (M = Co, Cu, Mn; BTC = 1,3,5-benzenetricarboxylate) MOF by supramolecular self-assembly.

The BTC anion is one of the best ligands for the design and construction of inorganic−organic-hybrid porous frameworks because of its thermal stability and symmetry. BTC and the hexaaquo metal complex ions $[M^{II}(H_2O)_6]^{2+}$ (M = Co, Cu, Mn) were chosen to illustrate the strategy of encapsulating the metal complex $[M^{II}(phen)_2(H_2O)_2]^{2+}$ into supramolecular frameworks through hydrogen bonding and $\pi-\pi$ interactions. Excellent channel-selective catalytic activities of these supramolecular compounds in the hydroxylation of phenols were observed, and maximum hydroquinone (HQ)/catechol (CAT) ratios of 3.6−3.9 were achieved.

Experimental Section

Physical Measurements. IR spectra were recorded using a Nexus-870 spectrophotometer. Elemental analysis for C, H, and N was performed using an Elementar Vario EL-III analyzer. Compositions of the metal elements for these compounds were analyzed using an ICPs-96B analyzer. Thermal gravimetric analysis (TGA) was performed under a static air atmosphere using a PerkinElmer 7 thermogravimetric analyzer with a heating rate of 5 °C min^{-1}. X-ray diffraction (XRD) measurements were performed using a Rigaku D/Max 3III diffractometer with a scanning rate of 4 deg min^{-1}. The products of the catalytic phenol hydroxylation reaction were analyzed using an Agilent 1200 liquid chromatograph with an IORBAX Eclipse XDB-C18 4.6 × 150 mm column, 7:3 methanol/water as the mobile phase, and UV−vis detection. HQ and CAT were defined qualitatively and quantitatively. Calculations of phenol conversion and product yield were based on the amount of phenol added.

Synthesis of the Compounds. $[Co(phen)_2(H_2O)_2]_2[Co(H_2O)_6]\cdot 2BTC\cdot 21.5H_2O$ (1). A solution of $[Co(phen)_2]Cl_2$ (1 mmol) in ethanol (10 mL) and an aqueous solution (10 mL) of $CoCl_2$ (0.5 mmol) were combined and added slowly with stirring to an aqueous solution (30 mL) of Na_3BTC (1 mmol). The resulting mixture was filtered, and orange cubic crystals of **1** suitable for X-ray diffraction formed from the filtrate after it stood for 3 weeks at room temperature. Yield {based on $[Co(phen)_2]Cl_2$}: 35%. **1** was insoluble in water and in common organic solvents. Anal. Calcd (%) for **1** ($C_{66}H_{101}Co_3N_8O_{43.5}$): C, 42.18; H, 5.417; N, 5.962; Co, 9.407. Found (%): C, 42.29; H, 5.169; N, 6.021; Co, 9.419. IR (KBr, cm^{-1}): 3410 (vs), 1620 (s), 1560 (s), 1430 (s), 1360 (s), 769 (m), 725 (s). The broad absorption peak at 3410 cm^{-1} indicated that a significant amount of H_2O was present in the compound. The absorption peaks at 1620 and 1560 cm^{-1} were assigned to the ν_{COO^-} asymmetric stretches of BTC, and the absorption peak at 1360 cm^{-1} was attributed to the BTC ν_{COO^-} symmetric stretch. The absorption peak at 1430 cm^{-1} was assigned to the stretching vibrations of the phenanthroline aromatic rings. The 769 and 725 cm^{-1} peaks corresponded to δ_{C-H} in phenanthroline.

$[Co(phen)_2(H_2O)_2]_2[Cu(H_2O)_6]\cdot 2BTC\cdot 21.5H_2O$ (2). This compound was prepared by a method similar to that for **1**, with $CuCl_2$ substituted for $CoCl_2$. The azure-colored cubic crystals of **2** were insoluble in water and in common organic solvents. Yield {based on $[Co(phen)_2]Cl_2$}: 34%. Anal. Calcd (%) for **2** ($C_{66}H_{101}Co_2CuN_8O_{43.5}$): C, 42.08; H, 5.404; N, 5.948; Co, 6.256; Cu, 3.373. Found (%): C, 42.17; H, 5.255; N, 6.033; Co, 6.235; Cu, 3.386. IR (KBr, cm^{-1}): 3410 (vs), 1620 (s), 1560 (s), 1430 (s), 1360 (s), 771 (m), 725 (s). The IR spectrum of the compound was similar to that of **1**, except that the phenanthroline C−H stretch was found at 771 cm^{-1} rather than 769 cm^{-1}.

$[Co(phen)_2(H_2O)_2]_2[Mn(H_2O)_6]\cdot 2BTC\cdot 18H_2O$ (3). This compound was also prepared by a method similar to that for **1**, with $MnCl_2$ substituted for $CoCl_2$. The orange-red cubic crystals of **3**were insoluble in water and in common organic solvents. Yield {based on $[Co(phen)_2]Cl_2$}: 39%. Anal. Calcd (%) for **3**($C_{66}H_{94}Co_2MnN_8O_{40}$): C, 43.74; H, 5.228; N, 6.183; Co, 6.503; Mn, 3.031. Found (%): C, 43.82; H, 4.961; N, 6.316; Co, 6.517; Mn, 3.024. IR (KBr, cm^{-1}): 3410 (vs), 1610 (s), 1560 (s), 1430 (s), 1360 (s), 773 (m), 725 (s). The IR spectrum of the compound was similar to that of **1**, except that the phenanthroline C−H stretch was found at 773 cm^{-1} rather than 769 cm^{-1}.

$[Zn(phen)_2(H_2O)_2]_2[Mn(H_2O)_6]\cdot 2BTC\cdot 22.5H_2O$ (4). This compound was also prepared by a method similar to that for **1**, with $MnCl_2$ and $[Zn(phen)_2]Cl_2$ substituted for $CoCl_2$ and $[Co(phen)_2]Cl_2$, respectively. The light-yellow cubic crystals of **4** were insoluble in water and in common organic solvents. Yield {based on $[Zn(phen)_2]Cl_2$}: 38%. Anal. Calcd (%) for **4** ($C_{66}H_{103}Zn_2MnN_8O_{44.5}$): C, 41.58; H, 5.446; N, 5.878; Zn, 6.860; Mn, 2.882. Found (%): C, 41.67; H, 5.152; N, 6.032; Zn, 6.873; Mn, 2.889. IR (KBr, cm^{-1}): 3410 (vs), 1620 (s), 1560 (s), 1430 (s), 1360 (s), 775 (m), 725 (s). The IR spectrum of the compound was similar to that of **1**, except that the phenanthroline C−H stretch was found at 775 cm^{-1} rather than 769 cm^{-1}.

Examination of Catalytic Activity. Catalytic activity measurements were carried out in a 50 mL glass reaction flask fitted with a condenser (circulating chilled water). Crystals of **1**, **2**, **3**, or **4** were ground in a mortar until they became a microcrystalline powder. Phenol or 1-naphthol (0.05 mol), 15 mL of ethanol, and the powder of **1**, **2**, **3**, or **4** (25 mg) were added to the flask. The mixture was heated to 30 or 40 °C with stirring. A solution of 30% aqueous H_2O_2 (0.05 mol) in 10 mL of water was then added dropwise over a period of about 0.5 h. The reaction was continued for an additional 7.5 h. The sample was removed and centrifuged to recover the solid catalyst, which was then washed alternately with distilled water and ethanol three times and dried in an oven at 40 °C. As a result, each catalyst recovered its activity and could be reused.

Crystallographic Data and Refinement of the Structures. The diffraction intensities of an orange cubic crystal of **1** were measured at 293(2) K using a Siemens SMART CCD area-detector diffractometer with graphite-monochromatized Mo Kα radiation (λ = 0.71073 Å). A total of 32 345 reflections were collected over the angle range $2.22° \le \theta \le 27.48°$; 9964 of these reflections were unique, with $R_{int} = 0.0535$. Corrections for Lp effects and empirical absorption were applied. The structure was solved using direct

(13) Sawaki, T.; Dewa, T.; Aoyama, Y. *J. Am. Chem. Soc.* **1998**, *120*, 8539–8540.
(14) Seo, J. S.; Whang, D.; Lee, H.; Jun, S. I.; Oh, J.; Jeon, Y. J.; Kimoon, K. *Nature* **2000**, *404*, 982–986.
(15) Xavier, K. O.; Chacko, J.; Mohammed Yusuff, K. K. *Appl. Catal., A* **2004**, *258*, 251–259.
(16) Mukhopadhyay, K.; Mandale, A. B.; Chaudhari, R. V. *Chem. Mater.* **2003**, *15*, 1766–1777.
(17) Alvaro, M.; Cardin, D. J.; Colquhoun, H. M.; Garcia, H.; Gilbert, A.; Lay, A. K.; Thorpe, J. H. *Chem. Mater.* **2005**, *17*, 2546–2551.
(18) Ganesan, R.; Viswanathan, B. *J. Phys. Chem. B* **2004**, *108*, 7102–7114.

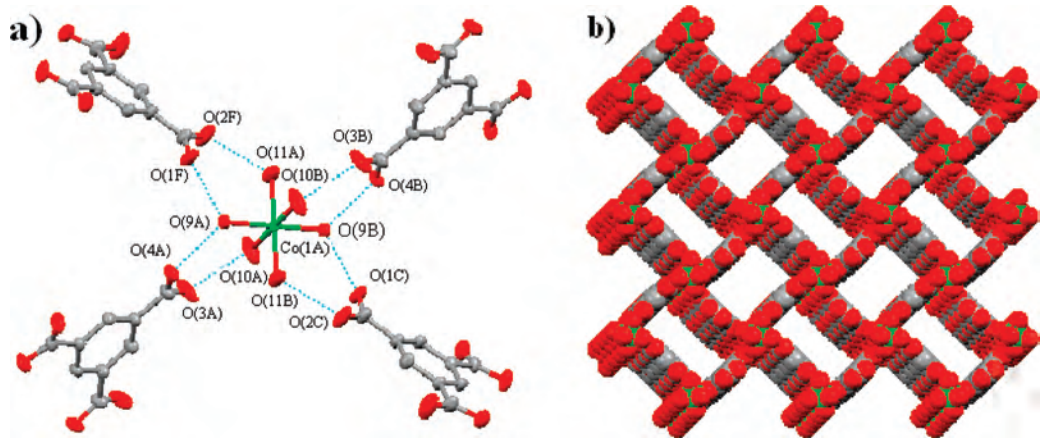

Figure 1. (a) View of the hydrogen-bonded repeating unit that forms the 2D hydrogen-bonded host framework of **1**. (b) Space-filling representation of the $[Co(H_2O)_6(BTC)_2]^{4-}$ 2D hydrogen-bonded host framework with rectangular-shaped cavities in **1**, showing 1D channels running along the *a* axis. $[Co(phen)_2(H_2O)_2]^{2+}$ and all of the free water molecules have been omitted for clarity. Color code: green, Co; red, O; gray, C. Symmetry codes: 1 and 2, $-x$, $y - {}^1/_2$, $-z + {}^1/_2$; 3 and 4, $-x$, $-y + 1$, $-z$.

Table 1. Summary of Crystallographic Data and Refinement Parameters for **1**−**4**

	1	**2**	**3**	**4**
empirical formula	$C_{66}H_{101}Co_3N_8O_{43.5}$	$C_{66}H_{101}Co_2CuN_8O_{43.5}$	$C_{66}H_{94}Co_2MnN_8O_{40}$	$C_{66}H_{103}Zn_2MnN_8O_{44.5}$
fw	1879.38	1883.95	1812.29	1906.24
cryst syst	monoclinic	monoclinic	monoclinic	monoclinic
space group	$P2_1/c$	$P2_1/c$	$P2_1/c$	$P2_1/c$
a (Å)	12.738(3)	12.7195(6)	12.748(3)	12.7807(10)
b (Å)	19.127(4)	19.0073(10)	18.983(4)	19.0571(13)
c (Å)	18.040(4)	18.0178(7)	18.061(4)	18.1501(10)
α (deg)	90	90	90	90
β (deg)	90.916(2)	90.046(2)	90.035(2)	90.170(5)
γ (deg)	90	90	90	90
V (Å^3)	4394.7(17)	4356.0(4)	4370.5(15)	4420.7(5)
ρ_{calcd} (g cm^{-3})	1.408	1.436	1.377	1.432
Z	2	2	2	2
μ (mm^{-1})	0.655	0.716	0.609	0.777
λ (Å)	0.71073	0.71073	0.71073	0.71073
T (K)	293 (2)	293 (2)	293 (2)	293 (2)
total reflns, unique reflns, R_{int}	32 345, 9964, 0.0535	33 101, 9928, 0.0241	33 096, 9956, 0.0508	32 377, 10 114, 0.0286
obsd [$I > 2.00\sigma(I)$]	9964	9928	9956	10 114
final R1, wR2[a]	0.0810, 0.2209	0.0680, 0.1874	0.0687, 0.1902	0.0592, 0.1785

[a] $R1 = \sum||F_o| - |F_c||/\sum|F_o|$ and $wR2 = [\sum w(F_o^2 - F_c^2)^2/\sum w(F_o^2)^2]^{1/2}$.

methods and expanded using Fourier techniques; SHELXS-97[19] was employed in the solution and refinement of the structure. The non-hydrogen atoms were refined anisotropically, while hydrogen atoms were added according to a theoretical model. Crystal data collection and structure refinement for **2**−**4** were carried out in a similar manner using Mo Kα radiation. Abbreviated crystal data and refinement parameters for **1**−**4** are given in Table 1.

Results and Discussion

Description of the Structures. The two different metal centers in these compounds could be distinguished by their molar ratios. Single-crystal X-ray structural analysis showed that the three-dimensional (3D) hydrogen-bonded framework of each compound consists of three parts: $[M^{II}(H_2O)_6]^{2+}$, BTC, and $[M^{II}(phen)_2(H_2O)_2]^{2+}$. Each hexaaquo metal complex ion, $[M^{II}(H_2O)_6]^{2+}$, is hydrogen bonded to four BTC ions via the carboxylate oxygen atoms of BTC and the hydrogen atoms of the coordinated water molecules of $[M^{II}(H_2O)_6]^{2+}$. In turn, each BTC ion bridges two $[M^{II}(H_2O)_6]^{2+}$ ions through these same hydrogen bonds (Figure 1a). This repeating unit forms an infinite two-dimensional (2D) framework $[M^{II}(H_2O)_6(BTC)_2]^{4-}$ (M = Co for **1**, Cu for **2**, Mn for **3**, **4**) with well-proportioned, rectangular-shaped cavities (17.9 × 13.3 Å for **1**, 17.7 × 13.5 Å for **2**, 17.6 × 13.2 Å for **3**, and 17.9 × 13.4 Å for **4**) forming one-dimensional (1D) channels along the *a* axis (Figure 1b). Selected hydrogen-bond distances are listed in Table 2.

In addition, guest molecules of the metal complex $[M^{II}(phen)_2(H_2O)_2]^{2+}$ are contained in the 2D hydrogen-bonded $[M^{II}(H_2O)_6(BTC)_2]^{4-}$ host framework, encapsulated in the 1D channels along the *a* axis. The coordinated water molecules of $[M^{II}(phen)_2(H_2O)_2]^{2+}$ are hydrogen-bonded to the carboxylate oxygen atoms of BTC, forming a chainlike structure (Figure 2). Selected hydrogen-bond distances of the complexes can be found in Table 2. Thus, 3D hydrogen-bonded frameworks with encapsulated metal complexes are formed (Figure 3). The frameworks contain several free water molecules (21.5 H_2O for **1** and **2**, 18 H_2O for **3**, and 22.5

(19) Sheldrick, G. M. *SHELXS-97 and SHELXL-97, Software for Crystal Structure Analysis*; Siemens Analytical X-ray Instruments Inc.: Madison, WI, 1997.

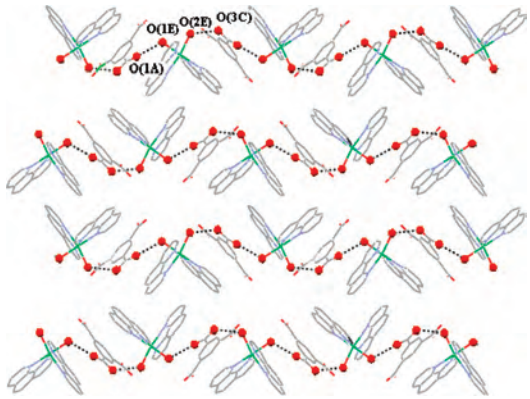

Figure 2. View of the 1D hydrogen-bonded chainlike structure of BTC and $[M^{II}(phen)_2(H_2O)_2]^{2+}$ (M = Co for **1**−**3**, Zn for **4**). Color code: green, Co; red, O; gray, C.

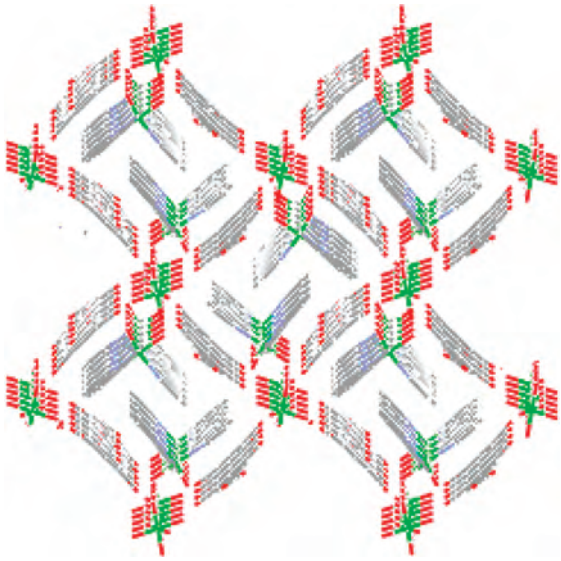

Figure 3. Molecular-packing diagram along the *a* axis for **1**, showing the hydrogen-bonding host−guest pattern and aromatic $\pi-\pi$ stacking interactions. All of the free water molecules are omitted for clarity. Color code: green, Co; red, O; gray, C.

Table 2. Selected Hydrogen-Bond Distances (Å) in Compounds **1**−**4**

hydrogen bond	1	2	3	4
O(3A)−O(10A)[a]	2.719	2.724	2.666	2.732
O(4A)−O(9A)[a]	2.667	2.653	2.729	2.662
O(3B)−O(10B)[a]	2.719	2.724	2.666	2.732
O(4B)−O(9B)[a]	2.667	2.653	2.729	2.662
O(1C)−O(9B)[b]	2.663	2.624	2.747	2.634
O(2C)−O(11B)[b]	2.750	2.740	2.636	2.748
O(1F)−O(9A)[b]	2.663	2.624	2.747	2.634
O(2F)−O(11A)[b]	2.750	2.740	2.636	2.748
O(1A)−O(1E)[c]	2.722	2.723	2.733	2.729
O(3C)−O(2E)	2.646	2.638	2.648	2.637

[a] Symmetry code: $-x, -y+1, -z$. [b] Symmetry code: $-x, y-1/2, -z+1/2$. [c] Symmetry code: $-x+1, y-1/2, -z+1/2$.

H_2O for **4**, in accordance with their formulas). After removal of these free water molecules, the void volume in the unit cell was estimated to be 1348 Å^3 (30.3% of the total volume) for **1**, 1345 Å^3 (30.2% of the total volume) for **2**, 1337 Å^3 (29.9% of the total volume) for **3**, and 1356 Å^3 (30.6% of the total volume) for **4**.[20]

Aromatic $\pi-\pi$ stacking interactions are also apparent in compounds **1**−**4**, as shown in Figure 3, and play a very important role in stabilizing the supramolecular structure.

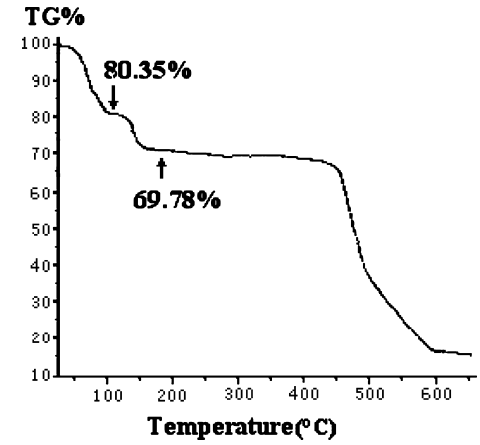

Figure 4. TGA curve for compound **1**.

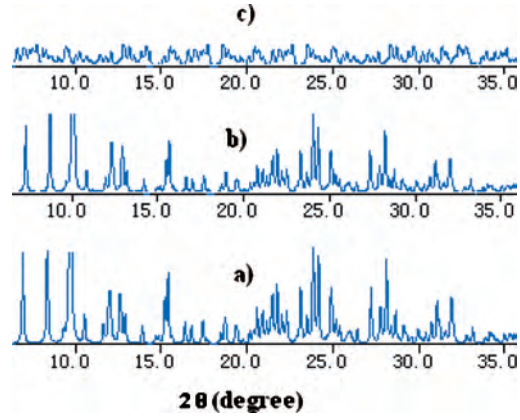

Figure 5. XRD patterns for **1**: (a) original crystal; (b) after baking at 80 °C for 2 h; (c) after baking at 140 °C for 2 h.

Plane-to-plane distances between phenanthroline molecules and the aromatic rings of neighboring BTC ions are 3.516 Å for **1**, 3.519 Å for **2**, 3.503 Å for **3**, and 3.512 Å for **4**, indicating significant aromatic $\pi-\pi$ stacking interactions between the phenanthroline molecules and the BTC aromatic rings.[21,22]

In order to study the thermal stabilities of these compounds, TGA was performed on polycrystalline samples of these materials in air at 1 atm pressure with a heating rate of 5 °C min^{-1}. This showed the loss of 21.5 free water guests per formula unit of **1** (a lost weight of 19.65%) over the temperature range 50−110 °C and the loss of 10 coordinated water molecules per formula unit (a lost weight of 10.57%) over the range 130−180 °C (Figure 4). XRD measurements also revealed that the 3D hydrogen-bonded framework of **1** was thermally stable below 80 °C but the interstitial water was partially lost, as can be deduced from changes in mass. When the temperature reached 140 °C, the lines broadened and their positions moved (Figure 5), indicating that the structure changed and the framework collapsed; thus, the elimination of interstitial water is not reversible. Similar TGA and XRD results were also obtained for compounds **2**−**4**.

(20) Spek, A. L. *J. Appl. Crystallogr.* **2003**, *36*, 7–14.
(21) Janiak, C. *J. Chem. Soc., Dalton Trans.* **2000**, 3885–3896.
(22) Zhang, X. M.; Tong, M. L.; Gong, M. L.; Chen, X. M. *Eur. J. Inorg. Chem.* **2003**, 138–142.

Table 3. Catalytic Hydroxylation of Phenols by H_2O_2 Using Compounds **1**−**4**[a]

	conversion (wt %)		HQ/CAT ratio	
catalyst	30 °C	40 °C	30 °C	40 °C
$Co(phen)_2Cl_2$	27.5	34.1	0.7	0.7
$Zn(phen)_2Cl_2$	20.6	26.4	0.6	0.6
1[b]	17.1	24.2	3.9	3.5
2[b]	16.8	23.7	3.7	3.2
3[b]	16.7	23.9	3.7	3.3
4[b]	14.8	20.2	3.6	3.2
1[c]	4.6	6.2	4.8	4.1

[a] Reaction conditions: phenol, 50 mmol; H_2O_2, 50 mmol; catalyst, 25 mg; solvent, ethanol/water; reaction time, 8 h. [b] Powdered crystals. [c] Original cubic crystals with dimensions of 0.1−0.2 mm.

Catalytic Properties. The most interesting feature of compounds **1**−**4** is that the 3D hydrogen-bonded frameworks include nanochannels, which are very important for highly channel selective catalysis. The catalytic activities of **1**−**4** were tested using hydroxylation of phenol or 1-naphthol by H_2O_2. In general, the products of hydroxylation of phenol are primarily HQ and CAT. Although many kinds of catalysts, such as metal oxides, metal complexes, zeolites, and zeolite-encapsulated metal complexes, have been developed for hydroxylation of phenols (and especially for oxidation of phenols), the HQ/CAT ratio generally is less than 1[23–26] except in the cases of a few zeolite-encapsulated catalysts.[27–29]

Reaction conditions of 30 °C for 8 h or 40 °C for 8 h were selected. In the absence of catalyst, hydroxylation of phenol or 1-naphthol using H_2O_2 yielded only trace products at 40 °C for 8 h. Hydroxylation of 1-naphthol catalyzed by compound **1**, **2**, **3**, or **4** at 40 °C for 8 h showed only about 3.4−3.8% conversion; for comparison, use of $Co(phen)_2Cl_2$ or $Zn(phen)_2Cl_2$ as the catalyst under the same reaction conditions produces 22.6 or 17.3% conversion of 1-naphthol, respectively. Such low conversion may be attributed to catalyzed hydroxylation occurring on the surface of the solid **1**, **2**, **3**, or **4** rather than in the channels of the framework, since the large size of the 1-naphthol molecule inhibits its diffusion into the channels. However, in the case of the smaller phenol molecule, which can freely diffuse into the framework channels, compounds **1**−**4** exhibited high catalytic activities for the hydroxylation reaction, with phenol conversions of 24.2, 23.7, 23.9, and 20.2%, respectively, at 40 °C. The large difference in the conversion of phenol as opposed to 1-naphthol under the same reaction conditions (Table 3) indicates significant size-selective catalysis.

As can be seen from Table 3, high phenol conversion was observed for homogeneous catalytic hydroxylation of phenols using $Co(phen)_2Cl_2$ or $Zn(phen)_2Cl_2$, but the HQ/CAT ratio was very low (0.7 or 0.6, respectively). Surprisingly and interestingly, compounds **1**−**4** showed a remarkably high HQ selectivity (with HQ/CAT ratios of 3.9, 3.7, 3.7, and 3.6, respectively, at 30 °C), and the HQ selectivity decreased slightly with an increase in reaction temperature. Such unique catalytic behavior is probably the result of heterogeneous catalysis, since compounds **1**−**4** scarcely dissolve in the reaction solution. In addition, the significantly shape-selective catalytic activities of **1**−**4** indicate that the hydroxylation reaction may have taken place in the channels of the supramolecular frameworks and that the formation and diffusion of CAT may have been constrained in the channels.[30] This is also supported by the significant effect of the crystal size of the catalyst on the catalytic hydroxylation of phenol using **1**. Hydroxylation of phenols by H_2O_2 using large cubic crystals of **1** with dimensions of 0.1−0.2 mm at 30 and 40 °C for 8 h resulted in phenol conversions of only 4.6 and 6.2%, respectively, which were much lower than the results obtained using powdered crystals of **1**. However, the HQ/CAT ratio increased dramatically, to a maximum of 4.8, suggesting that the reaction takes place primarily in the channels, with the longer diffusion paths in the larger-sized crystals leading to increased selectivity.

From Table 3, we see no obvious differences among the catalytic activities (respective phenol conversions of 24.2, 23.7, and 23.9% at 40 °C) of compounds **1**−**3**, which have the same $[Co(phen)_2(H_2O)_2]^{2+}$ guest but different host frameworks; however, the activity was significantly different for compound **4**, which has the same $[Mn(H_2O)_6(BTC)_2]^{4-}$ host framework as in **3** but $[Zn(phen)_2(H_2O)_2]^{2+}$ as the guest. Under the same conditions, the phenol conversion of **4** was only 20.2%, which was much less than that of **3**. This result indicates that the $[M^{II}(phen)_2(H_2O)_2]^{2+}$ complex encapsulated in the host framework was responsible for the catalytic hydroxylation of phenol and that in the reactions studied, the metal species in the host framework had no significant catalytic effect. Consequently, in this kind of catalyst, $[M^{II}(phen)_2(H_2O)_2]^{2+}$ is a significant catalytic activity center. In addition, when the reaction temperature was increased, conversion of phenol increased remarkably while the HQ/CAT ratio decreased slightly, because of the higher diffusion rates of the reactants and products in the framework channels.

Conclusions

In summary, we have synthesized four novel 3D microporous supramolecular compounds with nanosized channels and presented a synthetic strategy for self-encapsulating a metal complex as a catalytic activity center in a 3D porous framework. Under mild conditions, the metal complexes $[M^{II}(phen)_2(H_2O)_2]^{2+}$, which have high catalytic activities in the hydroxylation of phenols, were encapsulated in $[M^{II}(H_2O)_6(BTC)_2]^{4-}$ MOFs by self-assembly. Significant channel selectivity of these supramolecular compounds was found in the hydroxylation of phenols using H_2O_2, with a maximum HQ/CAT ratio of 3.9. Although this work is preliminary, it clearly demonstrates that the concept of

(23) Shevade, S. S.; Raja, R.; Kotasthane, A. N. *Appl. Catal., A* **1999**, *178*, 243–249.
(24) Seelan, S.; Sinha, A. K. *Appl. Catal., A* **2003**, *238*, 201–209.
(25) Jiang, Y.; Gao, Q. *Mater. Lett.* **2007**, *61*, 2212–2216.
(26) Choi, J. S.; Yoon, S. S.; Jang, S. H.; Ahn, W. S. *Catal. Today* **2006**, *111*, 280–287.
(27) Kerton, O. J.; McMorn, P.; Bethell, D.; King, F.; Hancock, F.; Burrows, A.; Kiely, C. J.; Ellwood, S.; Hutchings, G. *Phys. Chem. Chem. Phys.* **2005**, *7*, 2671–2678.
(28) Yube, K.; Furuta, M.; Aoki, N.; Mae, K. *Appl. Catal., A* **2007**, *327*, 278–286.
(29) Yube, K.; Furuta, M.; Mae, K. *Catal. Today* **2007**, *125*, 56–63.
(30) Chang, C. D.; Hellring, S. D. U.S. Patent 4,578,521, 1986.

encapsulating catalysts in supramolecular porous frameworks can be employed successfully as a strategy for designing and synthesizing new kinds of catalysts.

Acknowledgment. This work was financially supported as a key research project (06022020) of the Natural Science Foundation of Anhui Province, China. We thank Dr. Victoria Milway of the School of Chemistry, University of Manchester, U.K., for revising the manuscript.

Supporting Information Available: X-ray crystallographic data in CIF format for compounds **1**−**4**, water column arrays for these compounds, and figures illustrating how HQ is preferentially obtained with respect to CAT. This material is available free of charge via the Internet at http://pubs.acs.org. The CIF data have also been deposited with the Cambridge Crystallographic Data Center (CCDC) [CCDC nos. 607368 (**1**), 607366 (**2**), 607367 (**3**), and 646120 (**4**)]. Copies of this information may be obtained free of charge from the Director, CCDC, 12 Union Rd., Cambridge CB2 1EZ, U.K. (fax, +44-1223-336033; e-mail, deposit@ccdc.cam.ac.uk).

IC7022049